Available online at www.sciencedirect.com
ScienceDirect
Nuclear Instruments and Methods in Physics Research A 577 (2007) 734–740
NUCLEAR INSTRUMENTS & METHODS IN PHYSICS RESEARCH Section A
www.elsevier.com/locate/nima

Correction of respiratory motion for IMRT using aperture adaptive technique and visual guidance: A feasibility study

Ho-Hsing Chen[a,b], Jay Wu[c,*], Keh-Shih Chuang[a], Hsiang-Chi Kuo[a]

[a]*Department of Biomedical Engineering and Environmental Sciences, National Tsing-Hua University, Taiwan, ROC*
[b]*Department of Radiation Oncology, Taichung Veteran General Hospital, Taiwan, ROC*
[c]*Department of Radiological Technology, Central Taiwan University of Science and Technology, Taiwan, ROC*

Received 26 February 2007; received in revised form 30 March 2007; accepted 11 April 2007
Available online 14 April 2007

Abstract

Intensity-modulated radiation therapy (IMRT) utilizes nonuniform beam profile to deliver precise radiation doses to a tumor while minimizing radiation exposure to surrounding normal tissues. However, the problem of intrafraction organ motion distorts the dose distribution and leads to significant dosimetric errors. In this research, we applied an aperture adaptive technique with a visual guiding system to toggle the problem of respiratory motion. A homemade computer program showing a cyclic moving pattern was projected onto the ceiling to visually help patients adjust their respiratory patterns. Once the respiratory motion becomes regular, the leaf sequence can be synchronized with the target motion. An oscillator was employed to simulate the patient's breathing pattern. Two simple fields and one IMRT field were measured to verify the accuracy. Preliminary results showed that after appropriate training, the amplitude and duration of volunteer's breathing can be well controlled by the visual guiding system. The sharp dose gradient at the edge of the radiation fields was successfully restored. The maximum dosimetric error in the IMRT field was significantly decreased from 63% to 3%. We conclude that the aperture adaptive technique with the visual guiding system can be an inexpensive and feasible alternative without compromising delivery efficiency in clinical practice.

PACS: 87.56.−v

Keywords: Respiratory motion; Visual guidance; Intensity-modulated radiation therapy

1. Introduction

An ideal radiotherapy has to maximize the tumor control probability (TCP) and minimize the normal tissue complication probability (NTCP). The dose delivery to the target should thus be more accurate and conformal, while irradiation of normal tissues should be spared. For the targets located in the thorax and upper abdomen, the dose delivery is less accurate than those located in the head, neck, and pelvis due to respiratory motion. Therefore, correction of respiratory motion to minimize the position uncertainty is necessary.

To overcome the respiratory motion, margins around a clinical tumor volume (CTV) are extended to form a planning target volume (PTV), leading to more absorbed doses to the nearby normal tissues [1,2] and consequently increasing the NTCP. Lujan et al. [3] compared dose differences between the static dose distribution and convolved dose distribution considering the intratreatment organ motion due to breathing in a three-field liver tumor treatment. The dose differences can be up to 26% in the regions outside the CTV. Ten Haken et al. [4] indicated that if the PTV expansions for patient breathing can be eliminated effectively, the tumor dose can be elevated by 6–11 Gy and TCP can be improved by 6–10% as well.

For intensity-modulated radiation therapy (IMRT), nonuniform beam profiles are employed to provide desired radiation dosage and higher dose conformality to the

*Corresponding author. Tel.: +886 4 22391647x7104; fax: +886 4 22396762.
E-mail address: jwu@ctust.edu.tw (J. Wu).

0168-9002/$ - see front matter © 2007 Elsevier B.V. All rights reserved.
doi:10.1016/j.nima.2007.04.122

tumor volume while sparing normal tissue doses. However, the problem of intrafraction organ motion distorts the dose distribution and leads to substantial errors in dose delivery [5–8]. The severity is associated with the beam parameters and the pattern of organ motion. Furthermore, margin expansion causes optimization of dose distribution as a result of inverse treatment planning hard to achieve, potentially reducing the benefit of IMRT [9].

In the last few years, medical physicists have devoted much effort to solving the respiratory motion problem [10]. Several approaches have been proposed, which can be roughly categorized into four groups: the respiratory gating [11–13], breath hold [14,15], active breathing control [16–18], and respiratory synchronization [19–24]. Until now, most of the techniques have not been widely implemented in clinics. Even for the most popular one, the respiratory gating technique, only 12% of the health care facilities have the associated equipments [8]. Moreover, although the respiratory gating techniques can shrink the treatment margins without compromising the tumor dose, the tradeoff is prolonged treatment time, which inevitably decreases the patient throughput. These two obstacles further limit the use of respiratory motion correction techniques in most of the facilities.

Synchronization of the IMRT field with organ motion has been proposed as another on-going class of techniques. Keall et al. [22] demonstrated the feasibility. However, the success of this technique depends strongly on the regularity and reproducibility of patient's breathing patterns. Other studies use additional radiation modality to assist the tracking of the moving tumor [24], which might increase the potential risks of stochastic effects in the aspects of radiation protection.

In seeking a more efficient and inexpensive alternative, we proposed an aperture adaptive technique with visual guidance. The visual guiding system helps patients adjust their respiratory patterns. Once the respiratory motion becomes regular, the leaf sequence of a dynamic multileaf collimator (MLC) can be synchronized with the trajectory of the moving target. The purpose of this study is to reduce the dosimetric errors caused by respiratory motion during dose delivery without compromising treatment efficiency.

2. Methods

2.1. Synchronization

If target motion due to respiration can be depicted by a periodic function, it can be corrected by synchronizing MLC leaves with the moving pattern. The beam's eye view at any phase of breathing is thus always located on the target position. To realize the above concept, a Varian 2100EX linear accelerator (Varian Medical Systems, Palo Alto, CA, USA) with 120-leaf MLC was used in this study. The collimator was rotated by 90° so that the leaf motion was parallel to the target motion. Therefore, the target velocity can be superimposed onto the original leaf velocity.

The $(i+1)$th leaf position (X'_{i+1}) considering the target motion is defined by summation of the original leaf position (X_i), original moving distance (d_i), and amplitude of respiratory motion (d'_i):

$$X'_{i+1} = X_i + d_i + d'_i,$$
$$d'_i = \frac{V_b \times F_{mu}}{319 \times \dot{D}}, \quad (1)$$

where V_b is the velocity of organ motion due to breathing, F_{mu} is the monitor unit (MU) given in the radiation field, and $\dot{D}$ is the output dose rate of the linear accelerator. Once the moving velocity of the organ is given, the MU is proportional to the correction term, d'_i. On the contrary, if the dose rate is increased, the correction term is decreased. Note that the MLC leaves are controlled by a sequence file which contains a cyclic redundancy check (CRC) to maintain file integrity. Once the content of the file has been modified manually according to Eq. (1), the CRC value should be changed correspondingly.

2.2. Visual guidance of patient's respiratory motion

We developed a computer program, the Breath Control (Brecon), which shows a cyclic moving pattern to visually help patients adjust and reproduce their respiratory patterns (Fig. 1). The breathing pattern was first monitored using fluoroscopy studies with patients in a favorable and comfortable condition. The mean durations of inhalation and exhalation were measured and inputted into the Brecon software. A projector with a brightness of 2000 ANSI lumens and a contrast ratio of 2000:1 was set up. The Brecon software was then projected onto the ceiling of the treatment room where the image can be clearly seen by the patient lying on the couch.

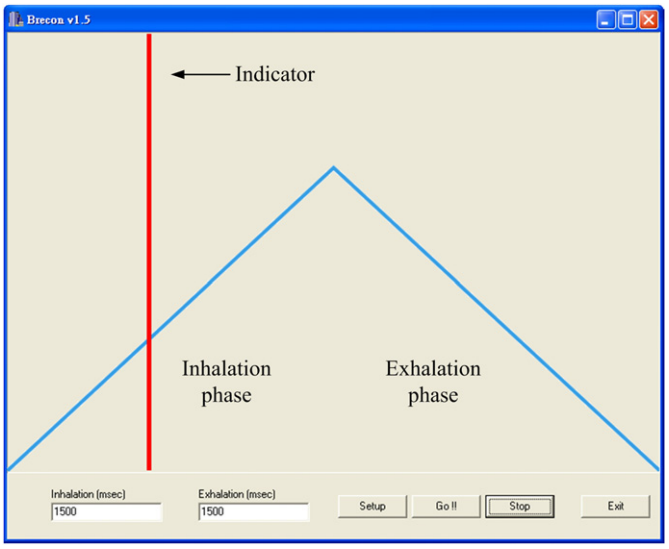

Fig. 1. The Brecon software displays a cyclic moving pattern to visually help patients adjust their respiratory patterns.

2.3. Simulating respiratory motion

An oscillator that uses high-pressure gas as a power source was employed to simulate the target motion due to respiration (Fig. 2). The platform of the oscillator was positioned at the machine isocenter perpendicular to the radiation beam. It can be horizontally moved along the moving direction of MLC leaves. Three phases of respiration including inhalation, exhalation, and hysteresis were simulated. The duration and amplitude of each phase can be adjusted separately by the extension and contraction control valves. The trajectory function of the oscillator is depicted in Fig. 3 with a range of approximately 2.5 cm and a period of 4 s, which represent the general target motion due to breathing.

2.4. Simple field measurements

Two simple fields of $4 \times 10\,cm^2$ including uniform and triangular dose distributions were created using the sliding window technique. Three configurations were compared, namely, the static beam and static target, static beam and moving target, and synchronized beam and moving target. The Kodak EDR2 film (Eastman Kodak Company, Rochester, NY, USA) was placed on the platform of the oscillator during measurements to verify the dose distribution of each situation. The exposed verification film was then scanned using a film digitizer (Kodak Lumiscan 50). Theoretically, the dose distribution after correction should be the same as the result of both the static beam and target configuration.

2.5. IMRT field measurements

A dynamic IMRT field for an abdomen treatment plan was employed to verify the aperture adaptive technique. Again, three different configurations were measured including the static beam and static target, static beam and moving target, and synchronized beam and moving target. Besides using V films, a solid water phantom (GAMMEX 473, GAMMEX RMI, USA) was positioned perpendicular to the beam. A total of seven points were measured using a PinPoint ionization chamber (Type 31006, PTW-Freiburg, Germany) at a depth of 5.0 cm of the solid water phantom.

2.6. Verifying effects of visual guiding system

The second part of this study was to examine the effects of regularizing the breathing pattern with the visual guiding system, Brecon. Eight volunteers from 18- to 35-years-old were selected in this trial. The real-time position management respiratory gating system (RPM) (Varian Medical Systems, Palo Alto, CA, USA) was used

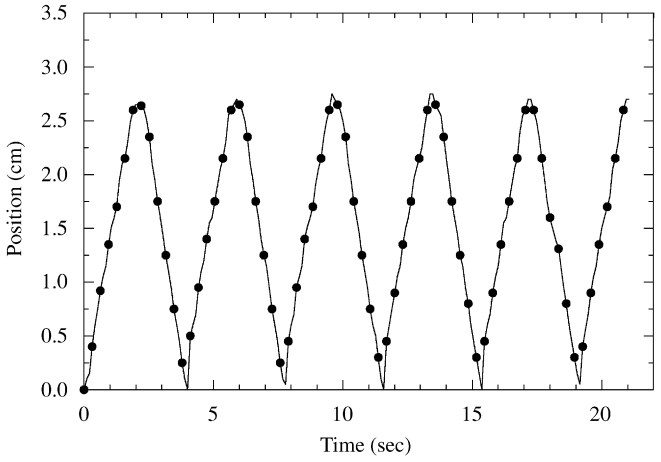

Fig. 3. The trajectory function of the oscillator with a range of approximately 2.5 cm and a period of 4 s.

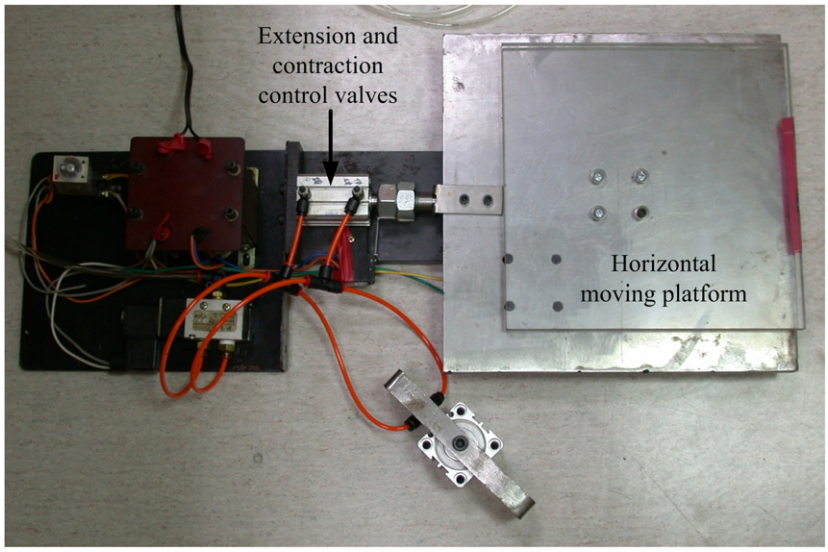

Fig. 2. The oscillator for simulating the target motion due to respiration. The platform was positioned perpendicular to the radiation beam.

as a monitor to record the respiratory motion of each volunteer. The mean inhalation and exhalation durations before visual guidance were calculated and then inputted into the Brecon as a gauge. After visual guidance, 3 min data were measured for each volunteer, and the last 150 s data were analyzed. Note that once the visual guiding system proves its effectiveness, additional management system for respiration could be spared during the treatment.

3. Results

Fig. 4 shows the fluence maps of the uniform field of $4 \times 10\,cm^2$ and the corresponding dose distributions before and after leaf synchronization, indicating that the sharp dose gradient at the edge was restored successfully. The central profiles are plotted in Fig. 5. The size of the penumbra with oscillation was increased from 3.7 to 15.1 mm. After correction, it was restored to 5.3 mm. Clinically, the radiation field is defined by the 50% iso-intensity contour. In this aspect, the three profiles in Fig. 5 show no difference. In fact, they are quite different from each other. Therefore, the 95% iso-intensity of the PTV was measured. The improvement was from 18.4 to 33.2 mm with the ideal value being 34.0 mm.

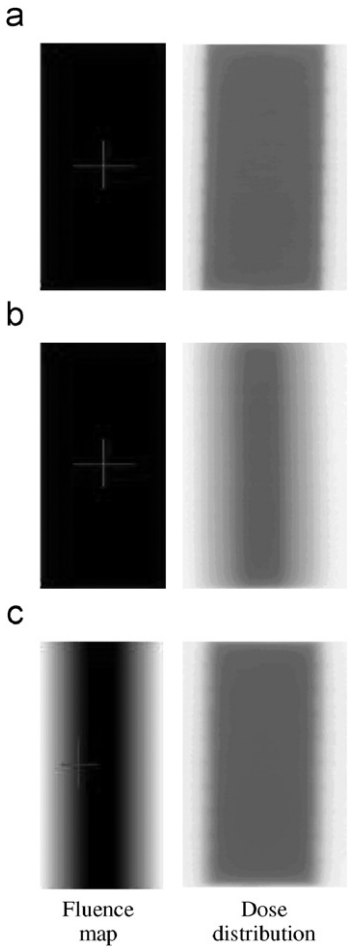

Fig. 4. The fluence maps and corresponding dose distributions of the uniform field with different configurations: (a) static beam and static target, (b) static beam and moving target, and (c) synchronized beam and moving target.

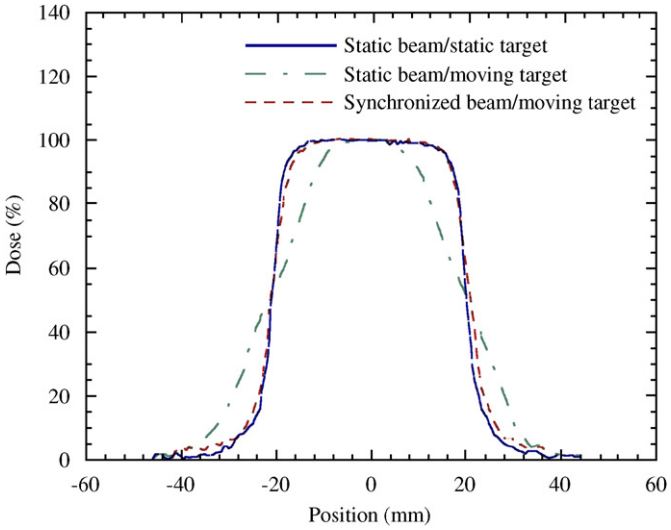

Fig. 5. The central horizontal profiles of the static beam and static target, static beam and moving target, and synchronized beam and moving target configurations of the uniform field.

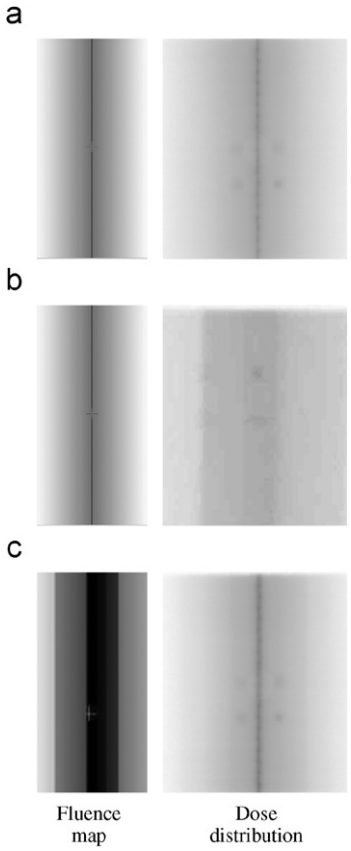

Fig. 6. The fluence maps and corresponding dose distributions of the triangular field with different configurations: (a) static beam and static target, (b) static beam and moving target, and (c) synchronized beam and moving target.

The fluence maps of the triangular field and the corresponding dose distributions are shown in Fig. 6, with their profiles displayed in Fig. 7. The uncorrected profile was irregular and was influenced by the moving pattern of the oscillator, whereas the corrected profile matched well with the one without target motion. Subsequently, the prescribed dose in the center of the radiation field can be achieved and the normal tissue dose can be spared.

The dose distributions for the IMRT field are illustrated in Fig. 8. As expected, the corrected dose map overcame the motion artifact which significantly destroyed the prescribed dose in the central vertical profile. The doses at seven locations are listed in Table 1, where the results were measured at a depth of 5.0 cm for 100 MU. When the correction was performed, the maximum dosimetric error significantly decreased from 63% to 3%. Note that locations 5 and 7 had the minimum errors compared with the static target condition. This is because the regions around these two locations have slight variations in the prescribed intensity. On the contrary, location 4 had the largest dose gradient, leading to the largest dosimetric error when the respiratory motion occurs.

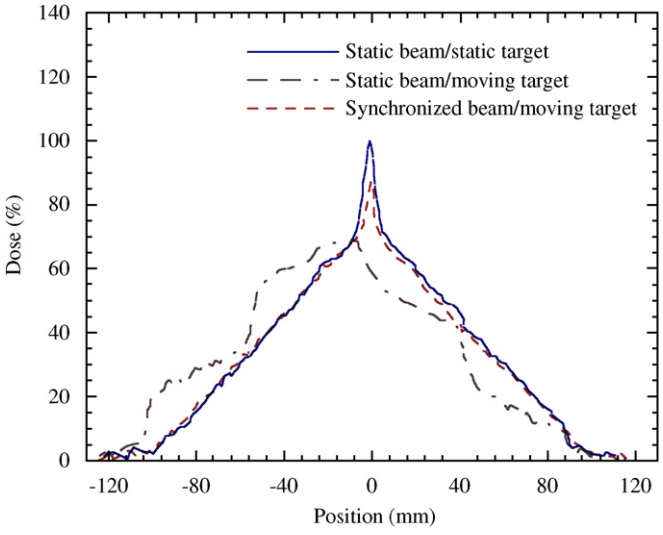

Fig. 7. The central horizontal profiles of the static beam and static target, static beam and moving target, and synchronized beam and moving target configurations of the triangular field.

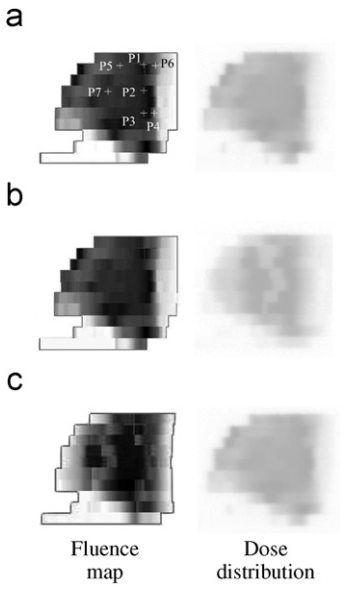

Fig. 8. The fluence maps and corresponding dose distributions for the IMRT field with different configurations: (a) static beam and static target, (b) static beam and moving target, and (c) synchronized beam and moving target. Seven locations marked in (a) were measured for their doses.

Table 1
Doses at seven locations of the IMRT filed. The results were measured at a depth of 5.0 cm for 100 MU

Location	Dose (cGy)		
	Static beam and static target	Static beam and moving target (percent error)	Synchronized beam and moving target (percent error)
1	82.9	44.7 (46%)	85.3 (2.9%)
2	96.3	37.5 (61%)	96.3 (0.0%)
3	98.5	42.3 (57%)	99.4 (0.9%)
4	44.2	16.3 (63%)	44.6 (0.9%)
5	76.6	83.4 (8.9%)	77.3 (0.9%)
6	57.3	24.0 (58%)	57.3 (0.0%)
7	85.9	88.4 (2.9%)	86.7 (0.9%)

The parameters of visual guidance and corresponding measurements are listed in Table 2. The mean duration of breathing cycle of each volunteer after applying visual guidance matched well with the duration of the visual guiding pattern. The mean percent error was reduced from 21% to 1.8%. The intrapatient standard deviations were significantly decreased as well. Although the mean ranges of the volunteers before and after using visual guidance were different, we found that the standard deviations decreased with visual guidance, which indicates that a more stable motion pattern can be achieved when a proper guiding system is used. Note that the volunteer 5 had the worst results because of the unsettled physical and mental conditions. This kind of patients should be excluded in advance from applying the aperture adaptive respiratory correction.

4. Discussion

The proposed aperture adaptive method with visual guidance synchronizes the leaf sequence with the organ motion by superimposing the amplitude of motion into the original leaf position. The method is applicable to both conformal field and IMRT field. Unlike the respiration gating techniques, this method does not waste any phase of the breathing cycle. Therefore, the treatment time does not need to be prolonged.

Before treatment, patients have to be trained for 10 min with the Brecon software. They have been told to follow

Table 2
Parameters of visual guidance and corresponding measurements for the eight volunteers

Volunteer	Parameters for Brecon		Before		After	
	Inhalation (ms)	Exhalation (ms)	Range (cm)	Duration (s)	Range (cm)	Duration (s)
1	2200	2000	1.33±13.4%	3.09±7.85%	1.54±9.10%	4.22±3.35%
2	3000	2300	0.75±16.0%	5.03±6.11%	1.34±11.1%	5.39±2.50%
3	3800	3800	1.84±3.64%	8.81±4.57%	1.68±2.43%	7.81±0.87%
4	2000	1800	0.69±11.4%	3.22±7.67%	1.20±6.55%	3.88±4.25%
5	2800	2500	0.71±7.71%	3.80±7.70%	1.60±14.0%	5.19±5.25%
6	2800	2500	1.21±6.91%	4.82±8.97%	1.30±3.97%	5.32±2.83%
7	1800	2200	0.83±16.1%	3.43±13.9%	2.30±7.77%	4.01±2.55%
8	3000	3000	1.41±14.6%	3.06±5.42%	2.98±5.80%	6.09±1.13%

the red indicator (Fig. 1) to adjust their breathing patterns. Those who have regular breathing patterns are selected for performing the correction procedure. Subsequently, the motion trajectory due to breathing can be depicted by the cyclic motion pattern. The success of this method therefore depends on the effectiveness of training and patient's cooperation. Moreover, the output of the linear accelerator should be stable enough so that the correction term of respiratory motion can be predicted accurately. An additional dose-rate monitor should therefore be used as a gauge for emergency beam off.

If the treatment is interrupted because of some unexpected situations, it should be possible to proceed with the treatment. For conformal therapy, the interrupted treatment can be restarted from the initial phase of respiration and the residual dose is then delivered to the target. However, for the IMRT field, the treatment must be resumed from the phase where it is stopped. Although the linear accelerator has the function of partial treatment, which can proceed with dose delivery from beam interruption, the respiration phase still needs to be recorded. Therefore, the visual guiding system should be directly connected to the linear accelerator. This is also the future work of our project.

At the beginning of dose delivery, the dose rate is relatively unstable due to mechanical instability. If this undesired period of time is prolonged, the synchronization will have a phase shift, causing failure of the proposed correction method. According to the quality assurance of linear accelerators, this period should be less than 0.2 s. We further analyzed the relative variation of the dose rate in this time frame, which is about 1% for the dose rate of 4 MU/min; and the corresponding variation in target motion is less than 0.1 mm. Compared with the amplitude of breathing pattern, this phase shift problem could be negligible, if the accelerator passes the quality assurance program.

In the dynamic mode of the VARIAN 2100EX linear accelerator, the dose rate can be defined manually. However, if the corresponding leaf velocity is over the limit of 2.5 cm/s, the system will automatically force the dose rate to decrease. For conformal therapy, the average target velocity due to breathing is approximately 1 cm/s, which is acceptable for the MLC. For the IMRT technique, the net velocity of each leaf is the vector sum of the original leaf velocity and target velocity, which might exceed the limitation. Therefore, the modified leaf sequence file should be tested before the treatment starts. If the velocity criterion is violated, we should revise the treatment plan by reducing the dose gradient to ensure the success of the treatment.

The proposed aperture adaptive technique and visual guiding system are applicable only if the patient's breathing pattern (cycle and amplitude) and accelerator's output parameters (MU and dose rate) are well known in advance and maintained constant during the course of treatment. In this study, a homemade software, Brecon, was developed for reproducing the breathing pattern of patients instead of using commercial products. The major advantage is low cost, which makes it possible for small and regional hospitals to adopt the correction of respiratory motion. Usually, it will take less than 20 min to evaluate whether a patient is suitable for the correction. Therefore, applying the proposed technique would have little impact on the workload of the RT center. We have proven the feasibility of using this visual guiding system on volunteers. Future studies would be focused on the real-time respiratory and dose-rate monitoring of patients to ensure greater accuracy in synchronization of the leaf sequence and target motion.

5. Conclusion

In this research, we developed an aperture adaptive technique with a visual guiding system to cope with the problem of target motion due to breathing. The leaf sequence is synchronized with the target motion so that the beam's eye view always focuses onto the target. An oscillator was employed to simulate the breathing pattern, and two simple fields and one IMRT field were measured to verify the accuracy of the proposed method. After correction, the sharp dose gradient at the edge of the radiation fields was successfully restored. The maximum dose error in the IMRT field was significantly decreased. Another key point in this study is the use of a cyclic moving pattern to depict the respiration pattern of patients. After appropriate training and visual guidance, the amplitude

and duration of volunteer's breathing can be well controlled by the Brecon software. We conclude that using the proposed aperture adaptive technique with the visual guiding system could be an inexpensive and practically achievable alternative without compromising treatment efficiency in clinical practice.

Acknowledgment

The authors would like to thank the National Science Council of Taiwan for financially supporting this research under Contract no. NSC92-2218-E-007-012.

References

[1] ICRU, Recording and reporting photon beam therapy, International Commission on Radiation Units and Measurements Report 50, 1993.
[2] ICRU, Recording and reporting photon beam therapy (supplement to ICRU Report 50), International Commission on Radiation Units and Measurements Report 62, 1999.
[3] A.E. Lujan, E.W. Larsen, J.M. Balter, R.K. Ten Haken, Med. Phys. 26 (1999) 715.
[4] R.K. Ten Haken, J.M. Balter, L.H. Marsh, J.M. Robertson, T.S. Lawrence, Int. J. Radiat. Oncol. Biol. Phys. 38 (1997) 613.
[5] G.D. Hugo, N. Agazaryan, T.D. Solberg, Med. Phys. 30 (2003) 1052.
[6] C.S. Chui, E. Yorke, L. Hong, Med. Phys. 30 (2003) 1736.
[7] S. Vedam, A. Docef, M. Fix, M. Murphy, P. Keall, Med. Phys. 32 (2005) 1607.
[8] J. Duan, S. Shen, J.B. Fiveash, R.A. Popple, I.A. Brezovich, Med. Phys. 33 (2006) 1380.
[9] A. Trofimov, E. Rietzel, H.M. Lu, B. Martin, S. Jiang, G.T. Chen, T. Bortfeld, Phys. Med. Biol. 50 (2005) 2779.
[10] P.J. Keall, G.S. Mageras, J.M. Balter, R.S. Emery, K.M. Forster, S.B. Jiang, J.M. Kapatoes, D.A. Low, M.J. Murphy, B.R. Murray, C.R. Ramsey, M.B. Van Herk, S.S. Vedam, J.W. Wong, E. Yorke, Med. Phys. 33 (2006) 3874.
[11] H.D. Kubo, B.C. Hill, Phys. Med. Biol. 41 (1996) 83.
[12] S.S. Vedam, P.J. Keall, V.R. Kini, R. Mohan, Med. Phys. 28 (2001) 2139.
[13] P. Giraud, E. Yorke, E.C. Ford, R. Wagman, G.S. Mageras, H. Amols, C.C. Ling, K.E. Rosenzweig, Lung Cancer 51 (2006) 41.
[14] G.S. Mageras, E. Yorke, Semin. Radiat. Oncol. 14 (2004) 65.
[15] S.S. Korreman, A.N. Pedersen, T.J. Nottrup, L. Specht, H. Nystrom, Radiother. Oncol. 76 (2005) 311.
[16] J.W. Wong, M.B. Sharpe, D.A. Jaffray, V.R. Kini, J.M. Robertson, J.S. Stromberg, A.A. Martinez, Int. J. Radiat. Oncol. Biol. Phys. 44 (1999) 911.
[17] E.M. Wilson, F.J. Williams, B.E. Lyn, J.W. Wong, E.G. Aird, Int. J. Radiat. Oncol. Biol. Phys. 57 (2003) 864.
[18] V.M. Remouchamps, N. Letts, D. Yan, F.A. Vicini, M. Moreau, J.A. Zielinski, J. Liang, L.L. Kestin, A.A. Martinez, J.W. Wong, Int. J. Radiat. Oncol. Biol. Phys. 57 (2003) 968.
[19] H. Shirato, M. Oita, K. Fujita, Y. Watanabe, K. Miyasaka, Int. J. Radiat. Oncol. Biol. Phys. 60 (2004) 335.
[20] H. Shirato, S. Shimizu, T. Kunieda, K. Kitamura, M. van Herk, K. Kagei, T. Nishioka, S. Hashimoto, K. Fujita, H. Aoyama, K. Tsuchiya, K. Kudo, K. Miyasaka, Int. J. Radiat. Oncol. Biol. Phys. 48 (2000) 1187.
[21] R. Onimaru, H. Shirato, M. Fujino, K. Suzuki, K. Yamazaki, M. Nishimura, H. Dosalca-Akita, K. Miyasaka, Int. J. Radiat. Oncol. Biol. Phys. 63 (2005) 164.
[22] P.J. Keall, V.R. Kini, S.S. Vedam, R. Mohan, Phys. Med. Biol. 46 (2001) 1.
[23] T. Neicu, H. Shirato, Y. Seppenwoolde, S.B. Jiang, Phys. Med. Biol. 48 (2003) 587.
[24] T. Zhang, R. Jeraj, H. Keller, W. Lu, G.H. Olivera, T.R. McNutt, T.R. Mackie, B. Paliwal, Med. Phys. 31 (2004) 1576.